MATHEMATICA MONTISNIGRI
Vol XLI (2018)

ELECTRICAL CONDUCTIVITY OF STRONGLY CORRELATED PLASMA MEDIA

V. S. FILINOV[1] AND A. S. LARKIN[1,2]

[1] Joint Institute for High Temperatures of the Russian Academy of Sciences
Izhorskaya 13 Bldg 2, 125412 Moscow, Russia
e-mail: vladimir_filinov@mail.ru

[2] Moscow Institute of Physics and Technology
Institutskiy Pereulok 9, 141700 Dolgoprudny, Moscow Region, Russia

Summary. According to the Kubo formula we study the electrical conductivity of dense plasma by a new quantum dynamics method in the Wigner representation of quantum mechanics. This method combines the Feynman and Wigner formulation of quantum mechanics and uses for calculation the direct path integral Monte Carlo (PIMC) and molecular dynamics methods. Namely we solve the Wigner–Liouville equation for dense degenerate plasma with the initial condition sampled by the PIMC method from equilibrium plasma state. We report calculation of the plasma conductivity and find agreement with available theories, simulations, experimental data and interpolation formula obtained by Esser, Redmer and Röpke.

1 INTRODUCTION

During the last decade, much work has been devoted to study the thermodynamic and kinetic properties of strongly coupled plasmas. In these works results were obtained either by numerical simulations or by analytical or semi-analytical calculations. Plasma is quantum mechanical even at high temperature and low density since the Heisenberg uncertainty principle is necessary to keep the electrons from collapsing into the ions, thus it cannot be described in the framework of classical mechanics. Nevertheless the classical molecular dynamics simulation became a traditional way of calculation of thermodynamic and transport properties of non-ideal plasmas [1–6]. The main difficulty, however, since the invention of Monte Carlo and molecular dynamics methods remains the treatment of bound states in dense media. As this is a quantum-mechanical or quantum-statistical problem more complex simulation approaches should be used such as density functional theory (DFT) [7–9] or path integral Monte Carlo (PIMC). This is the reason for classical methods with quantum-mechanical treatment of bound states to be used together with first-principle ones.

Electrical conductivity is one of the important quantities which determines the behavior of plasma. Knowledge of this fundamental value is important under interaction of charged particles or radiation with plasma, and, in particular, for the inertial thermonuclear fusion. Experimental efforts for the measurement of the electrical conductivity up to high densities revealed

2010 Mathematics Subject Classification: 81Q30, 81Q65, 82C10.
Key words and phrases: electrical conductivity, Kubo formula, Wigner representation, Monte Carlo.

the many quantum effects such as Pauli blocking, dynamic screening and self-energy, structure factor, the Debye–Onsager relaxation effect, formation of bound states etc. There are many theoretical models of dynamic conductivity which can be derived from the approximate solution of kinetic equations [1, 10–13]. Molecular dynamics simulations of fully ionized classical plasma are widely used for the calculation of electrical conductivity with the help of the Kubo formula [10], but our main interest is to improve these results by taking into account bound states and quantum exchange-correlation effects. This can be done by means of DFT theory, but it treats exchange-correlation effects approximately and can not be applied at high temperatures. Although different methods have been proposed for the evaluation of plasma transport properties [1, 11–18], it still remains a theoretical challenge to treat these effects by a unified quantum-statistical approach.

On other hand, Feynman and Wigner formulation of quantum mechanics combining with Monte Carlo methods is free from mentioned drawbacks and therefore can be used for construction of the generalized molecular dynamics method for the calculation of electrical conductivity of quantum strongly coupled plasmas. Here we describe the computational method which have been used for the calculation of electrical conductivity of dense plasma. To calculate the electrical conductivity we use quantum dynamics in the Wigner representation of quantum mechanics. The Wigner–Liouville equation is solved by a combination of molecular dynamics (MD) and PIMC methods. The initial conditions are obtained using PIMC which allow to calculate such thermodynamic quantities as the internal energy, pressure and pair distribution functions in a wide range of density and temperature. To study the influence of the interparticle interaction on the dynamic properties of dense plasmas we apply the quantum dynamics in the canonical ensemble at finite temperature and compute temporal momentum-momentum correlation functions and electrical conductivity. For low density and high temperature our numerical results agree well with interpolation formula, which is applicable for fully ionized plasma [17,18]. Our calculations agree also with experimental results for conductivity within wide region of plasma temperatures and densities [3].

2 WIGNER QUANTUM DYNAMICS

To calculate the electrical conductivity of dense two component Coulomb system of particle we use quantum dynamics in the Wigner representation of quantum mechanics. As example of Coulomb system of particles, we consider a 3D two-component mass asymmetric electron–hole plasma consisting of N_e electrons and N_h heavier holes in equilibrium ($N_e = N_h = N$) [19]. The Hamiltonian of the system $\hat{H} = \hat{K} + \hat{U}^c$ contains the kinetic energy $\hat{K}$ and the Coulomb interaction energy $\hat{U}^c = \hat{U}^c_{\rm hh} + \hat{U}^c_{\rm ee} + \hat{U}^c_{\rm eh}$ contributions.

Our starting point is the canonical ensemble-averaged time correlation function [10]

$$C_{FA}(t) = \left\langle \hat{F}(0)\hat{A}(t) \right\rangle = Z^{-1}\mathrm{Tr}\left\{ \hat{F}\mathrm{e}^{\mathrm{i}\hat{H}t_c^*/\hbar}\hat{A}\mathrm{e}^{-\mathrm{i}\hat{H}t_c/\hbar} \right\}, \tag{1}$$

where $\hat{F}$ and $\hat{A}$ are operators of arbitrary observables, $t_c = t - i\hbar\beta/2$ is the complex time, $\beta = 1/k_BT$ and $Z = \mathrm{Tr}\left\{ \mathrm{e}^{-\beta\hat{H}} \right\}$ is the partition function. The Wigner representation of (1) in a υ–dimensional space is

$$C_{FA}(t) = (2\pi\hbar)^{-2\upsilon}\int\int \mathrm{d}\overline{pq}\,\mathrm{d}\widetilde{pq}\,F(\overline{pq})\,A(\widetilde{pq})\,W(\overline{pq};\widetilde{pq};t;\beta), \tag{2}$$

where p and q comprise the momenta and coordinates of all particles, $\nu = 12N$. $A(\overline{pq})$ and $F(\widetilde{pq})$ denote the Weyl's symbols of the operators

$$A(pq) = \int \mathrm{d}\xi\,\mathrm{e}^{-\mathrm{i}\frac{p\xi}{\hbar}}\left\langle q - \frac{\xi}{2}\left|\hat{A}\right|q + \frac{\xi}{2}\right\rangle,$$

and $W(\overline{pq};\widetilde{pq};t;\beta)$ is the spectral density expressed as

$$W(\overline{pq};\widetilde{pq};t;\beta) = \frac{1}{Z}\int\int \mathrm{d}\bar{\xi}\,\mathrm{d}\tilde{\xi}\,\mathrm{e}^{\mathrm{i}\frac{\bar{p}\bar{\xi}}{\hbar}}\mathrm{e}^{\mathrm{i}\frac{\tilde{p}\tilde{\xi}}{\hbar}}\left\langle \bar{q} + \frac{\bar{\xi}}{2}\left|\mathrm{e}^{\mathrm{i}\hat{H}t_c^*/\hbar}\right|\tilde{q} - \frac{\tilde{\xi}}{2}\right\rangle\left\langle \tilde{q} + \frac{\tilde{\xi}}{2}\left|\mathrm{e}^{-\mathrm{i}\hat{H}t_c/\hbar}\right|\bar{q} - \frac{\bar{\xi}}{2}\right\rangle.$$

As has been proved in [20–22], W obeys the following integral equation:

$$\begin{aligned} W(\overline{pq};\widetilde{pq};t;\beta) = {} & \int \mathrm{d}\overline{p_0q_0}\,\mathrm{d}\widetilde{p_0q_0}\,G(\overline{pq},\widetilde{pq},t;\overline{p_0q_0},\widetilde{p_0q_0},0)\,W(\overline{p_0q_0};\widetilde{p_0q_0};t=0,\beta) \\ & + \frac{1}{2}\int_0^t \mathrm{d}t'\int \mathrm{d}s\int \mathrm{d}\overline{p'q'}\,\mathrm{d}\widetilde{p'q'}\,G\left(\overline{pq},\widetilde{pq},t;\overline{p'q'},\widetilde{p'q'},t'\right) \\ & \times\left[W(\overline{p}'-s,\overline{q}';\widetilde{p'q'};t';\beta)\,\omega(s,\overline{q}') - W(\overline{p'q'};\widetilde{p}'-s,\widetilde{q}';t';\beta)\,\omega(s,\widetilde{q}')\right], \end{aligned} \tag{3}$$

with the Green function

$$\begin{aligned} G\left(\overline{pq},\widetilde{pq},t;\overline{p'q'},\widetilde{p'q'},t'\right) = {} & \delta\left(\overline{p}-\overline{p}(t;\overline{p'q'},t')\right)\delta\left(\overline{q}-\overline{q}(t;\overline{p'q'},t')\right) \\ & \times\delta\left(\widetilde{p}-\widetilde{p}(t;\widetilde{p'q'},t')\right)\delta\left(\widetilde{q}-\widetilde{q}(t;\widetilde{p'q'},t')\right), \end{aligned}$$

describing propagation of the spectral density along classical trajectories in positive time direction

$$\frac{\mathrm{d}\overline{p}(t;\overline{p'q'},t')}{\mathrm{d}t} = \frac{1}{2}F(\overline{q}_t), \quad \frac{\mathrm{d}\overline{q}(t;\overline{p'q'},t')}{\mathrm{d}t} = \frac{1}{2}\overline{v}[\overline{p}(t;\overline{p'q'},t')], \tag{4}$$

and in the reverse time direction

$$\frac{\mathrm{d}\widetilde{p}(t;\widetilde{p'q'},t')}{\mathrm{d}t}=-\frac{1}{2}F(\widetilde{q}_t),\quad \frac{\mathrm{d}\widetilde{q}(t;\widetilde{p'q'},t')}{\mathrm{d}t}=-\frac{1}{2}\widetilde{v}[\widetilde{p}(t;\widetilde{p'q'},t')], \tag{5}$$

where $(\widetilde{q}_t)=[\widetilde{q}(t;\widetilde{p'q'},t')]$ and similarly for bared quantities, while vector v symbolize the particle velocities. These equations of motion are supplemented by the initial conditions at time $t=0$

$$\begin{aligned}\overline{p}(0;\overline{p_0q_0},0)&=\overline{p_0},\quad \overline{q}(0;\overline{p_0q_0},0)=\overline{q_0},\\ \widetilde{p}(0;\widetilde{p_0q_0},0)&=\widetilde{p_0},\quad \widetilde{q}(0;\widetilde{p_0q_0},0)=\widetilde{q_0},\end{aligned} \tag{6}$$

and by the initial conditions at time $t=t'$

$$\begin{aligned}\overline{p}(t';\overline{p'q'},t')&=\overline{p}',\quad \overline{q}(t';\overline{p'q'},t')=\overline{q}'.\\ \widetilde{p}(t';\widetilde{p'q'},t')&=\widetilde{p}',\quad \widetilde{q}(t';\widetilde{p'q'},t')=\widetilde{q}'.\end{aligned} \tag{7}$$

In fact, equations (4) are Hamiltonian equations of motion but written for half-time $(t/2)$. Similarly, equations (5) are half-time Hamiltonian equations of motion reversed in time. This happens because the time correlation is taken between instants in the past and the future with the initial conditions fixed in between these instants, i.e. at $t=0$ the spectral density is $W(\overline{pq}_0;\widetilde{pq}_0;t=0,\beta)=\bar{W}^0(\overline{pq}_0;\widetilde{pq}_0;\beta)$. The right-hand sides of equations (4) and (5) include interparticle interaction that can be arbitrary strong.

The solution of the integral equation (3) can be represented by an iteration series

$$W^t=\bar{W}^t+K^t_\tau W^\tau=K^t_0\bar{W}^0+K^t_{\tau_1}K^{\tau_1}_0\bar{W}^0+\ldots,$$

where $\bar{W}^t$ is the initial quantum spectral densities evolving classically during time intervals $[0,t]$, whereas $K^{\tau_{i+1}}_{\tau_i}$ are operators that govern the propagation from time τ_i to τ_{i+1} like the first term in equations (3) and momentum jumps due to the convolution structure of the equation (3), see e.g. [20–22]. Thus the time correlation function becomes

$$C_{FA}(t)=\left(\phi|W^t\right)=\left(\phi|\bar{W}^t\right)+\left(\phi|K^t_{\tau_1}K^{\tau_1}_0\bar{W}^0\right)+\ldots, \tag{8}$$

where $\phi(\overline{pq};\widetilde{pq})\equiv F(\overline{pq})A(\widetilde{pq})$ and the parentheses $(\ldots|\ldots)$ denote integration over the phase spaces $\{\overline{p_0q_0};\widetilde{p_0q_0}\}$, $\{d\overline{p'q'}\,d\widetilde{p'q'}\}$ and so on. To compute the electron electrical conductivity we calculate the electron momentum-momentum time correlation function $C_{pp}(t)$ and then apply the Kubo formula which contains the Fourier transform of $C_{pp}(t)$ at $\omega=0$.

The iteration series for $C_{FA}(t)$ can be efficiently computed using MC methods. We have developed a MC scheme which provides domain sampling of the terms giving the main contribution to the iteration series, cf. [20–22]. For simplicity, in this work, we take into account only the first term of iteration series, which is related to the propagation of the initial quantum distribution $\bar{W}^0$ according to the Hamiltonian equations of motion. This term, however, does not describe pure classical dynamics but accounts for quantum effects [20] and, in fact, contains arbitrarily high powers of the Planck's constant:

$$W(\overline{pq};\widetilde{pq};t;\beta) \simeq \int \mathrm{d}\overline{p_0q_0}\,\mathrm{d}\widetilde{p_0q_0}\,G(\overline{pq},\widetilde{pq},t;\overline{p_0q_0},\widetilde{p_0q_0},0) \times W^0(\overline{pq}_0;\widetilde{pq}_0;\beta). \tag{9}$$

Here the initial condition $\bar{W}^0(\overline{pq};\widetilde{pq};\beta) \equiv W(\overline{pq};\widetilde{pq};0;\beta)$ for equation (3) can be presented in the form of a finite difference approximation of the Feynman path integral [13, 21, 22].

The expression for W has to be generalized to account for the spin effects. This gives rise to an additional spin part of the initial density matrix, e.g. [23,24]. Also, to improve the simulation accuracy the pair interactions U_{ab}, are replaced by an effective quantum potential $U_{\mathrm{ab}}^{\mathrm{eff}}$, such as the Kelbg potential [25]. For details we refer to Refs. [13], where recent applications of the PIMC approach to correlated Coulomb systems has been discussed.

3 TRANSPORT COEFFICIENTS

A natural way to obtain transport coefficients is use of the quantum Green-Kubo relations [10]. These relations give the transport coefficients in terms of integrals of equilibrium time-depended correlation functions. According to equation (8) the electron conductivity σ is the integral of the velocity–velocity autocorrelation function

$$\sigma_e = e^2 n_e \beta \lim_{t\to\infty} \frac{1}{3}\int_0^t \mathrm{d}\tau \langle v(0)\cdot v(\tau)\rangle_e$$
$$\langle v(0)\cdot v(\tau)\rangle_e = (2\pi\hbar)^{-2\nu}\int \mathrm{d}\overline{pq}\,\mathrm{d}\widetilde{pq}\,W(\overline{pq};\widetilde{pq};\tau;\beta)\; v_e(\overline{p}(\tau))\cdot v_e(\widetilde{p}(\tau)), \tag{10}$$

where the scalar product of 3D velocities is

$$v_e(\overline{p}(\tau))\cdot v_e(\widetilde{p}(\tau)) = \frac{1}{N_e}\sum_{i=1}^{N_e}\frac{\overline{\mathbf{p}}_i(\tau)\cdot\widetilde{\mathbf{p}}_i(\tau)}{m_i^2}, \tag{11}$$

and trajectories in positive (bared) and inverse (tilded) time directions are defined by the equations (4) and (5), respectively.

Calculations of autocorrelation functions are performed in canonical ensemble and include

combination of the Monte-Carlo sampling of initial conditions $\overline{pq}_0$ and $\widetilde{pq}_0$ for trajectories and solving the system of dynamic Hamiltonian equations (4 and (5). The initial conditions $\overline{pq}_0$ and $\widetilde{pq}_0$ for the trajectories are sampled by the Monte-Carlo method accordingly to the modulus of probability $W^0(\overline{pq}_0;\widetilde{pq}_0;\beta)$, while sign of the $W^0(\overline{pq}_0;\widetilde{pq}_0;\beta)$ is accounted for as wiehgt function at calculations average values [13].

The autocorrelator (11) as a function of time is calculated along the trajectories (4) and (5), which themselves are computed by means of a numerical scheme for solution of a system of ordinary differential equations of the first order. We use the explicit numerical scheme with automatically adapted time step. To check correctness of the calculations we control the full energy. Energy variations in our calculations amount to less than 1-2%. Usually several thousands of generated trajectories are required for convergence of the antiderivative of the autocorrelation function up to accuracy of 5%. The convergence is fast enough because the autocorrelation function includes averaging-out (i.e. summation) over all particles.

Details of our path integral Monte-Carlo simulations have been discussed elsewhere in a number of papers and review books, see, e.g. Refs. [5, 13] and references therein. For simulation we use the standard Metropolis algorithm. We use a cubic simulation box with periodic boundary conditions. The main idea of the simulations consists in constructing a Markov chain of different particle states in the phase space.

Errors of Monte-Carlo calculations of thermodynamic quantities related to the finite particle number (N) in the system with periodic boundary conditions are of the order of $1/N$ [5]. However, too large number of particles presented by discrete trajectories with a large number of 3D points (beads) requires too large computer resources. In practical calculations we try to keep the total number of particles not exceeding $N = 126$ and the number of beads $n = 20$ for each particle is used. Our choice of particle and bead numbers is a compromise between acceptable accuracy and available computer resources. It was checked that variation of the number of beads from 15 up to 50 practically does not change results.

To avoid the well known sign problem in our Monte-Carlo simulations of Fermi particles we used the effective pair pseudopotential depending on coordinates, momenta and degeneracy parameter of particles and taking into account Pauli blocking of fermions in phase space. The agreement between the our calculations and the analytical Fermi distributions is good enough up to parameter of the electron degeneracy equal to $n\lambda_e^3 = 10\,(T/E_F = 0.141)$, while the integral characteristics such as energy are practically equal to each other [13, 23]. The degeneracy of electrons in our calculations is moderate, i.e. the degeneracy parameter is of order of several units.

4 ELECTRICAL CONDUCTIVITY

The plasma density is characterized by the Brueckner parameter r_s defined as the ratio of the mean interparticle distance of electrons $d = (\frac{3}{4\pi n_e})^{1/3}$ to the Bohr radius a_B (n_e is the electron densities). To estimate interaction and degeneracy effects we use the coupling $\Gamma = e^2/(r_s a_B k_B T)$ and the degeneracy $\chi = n_e \lambda_e^3$ parameters where $\lambda_e = 2\pi\hbar^2/(m_e k_B T)$ and m_e is the electron mass.

First we discuss the velocity–velocity auto correlation function (VVACF). Figure 1 shows examples of the velocity–velocity autocorrelation functions and its antiderivatives. The initail Wigner distribution $\bar{W}^0$ due to the path integral representation accounts for the momentum–coordinate principle uncertanity [13]. As consequence momenta are to a great extent independent form each other and VVACF approach to zero. Some time later correlation of VVACF starts to grow due to strong interaction with surrounding particles. This happens as $\Gamma_e \leqslant 1$, $|\overline{q_0} - \widetilde{q_0}| \sim \lambda_e$ and $\lambda_e \leqslant \beta e^2 \leqslant r_s a_B$ and virtual trajectories $\overline{pq}$ and $\widetilde{pq}$ are evolving in approximately same direction independently from initial conditions. Subsequent decay of VVACF results from interaction with far particles at distances larger than r_s. Accordung to figure 1 the damping time of the VVACF turns out to be strongly affected by the variations of density and temperature.

Let us discuss now the conductivity of a strongly coupled Coulomb system. Top panel of figure 2 present comparison of our conductivity isochores with those obtained from the interpolation formula for conductivity of fully ionized hydrogen plasma derived in [17, 18]. This figure demonstrates good agreement of both data at low densitis and high temperatures. Let us stress that line 6 restricts approximately from above the region of conductivity sharp drop due to arising bound states of many particle clusters.

Bottom panel of figure 2 presents (by solid symbols) the Coulomb part of electron conductivity obtained in experiments for different substances, densities and temperatures versus coupling plasma parameter Γ_e. Line 1 illustrate conductivity of MD calculations [27], while lines 2 and 3 show conductivity for ideal plasma. Empty symbols 1–5 preset results obtained in this work for five fixed densities related to $r_s = 6, 4, 3, 2, 1$, while symbols $6, 7$ present results of theoretical papers [3] and [26] for fully ionized hydrogen plasma. Important difference with classical molecular dynamics is that even for fully ionized plasma (proved by related behavior of PIMC pair distribution functions) we can see stratification of conductivity isochores for related fixed Brackner parameter. This happens due to the accounting for quantum effects even at small coupling parameter and high temperatures. This stratification is also supported by experimental results presented by solid symbols.

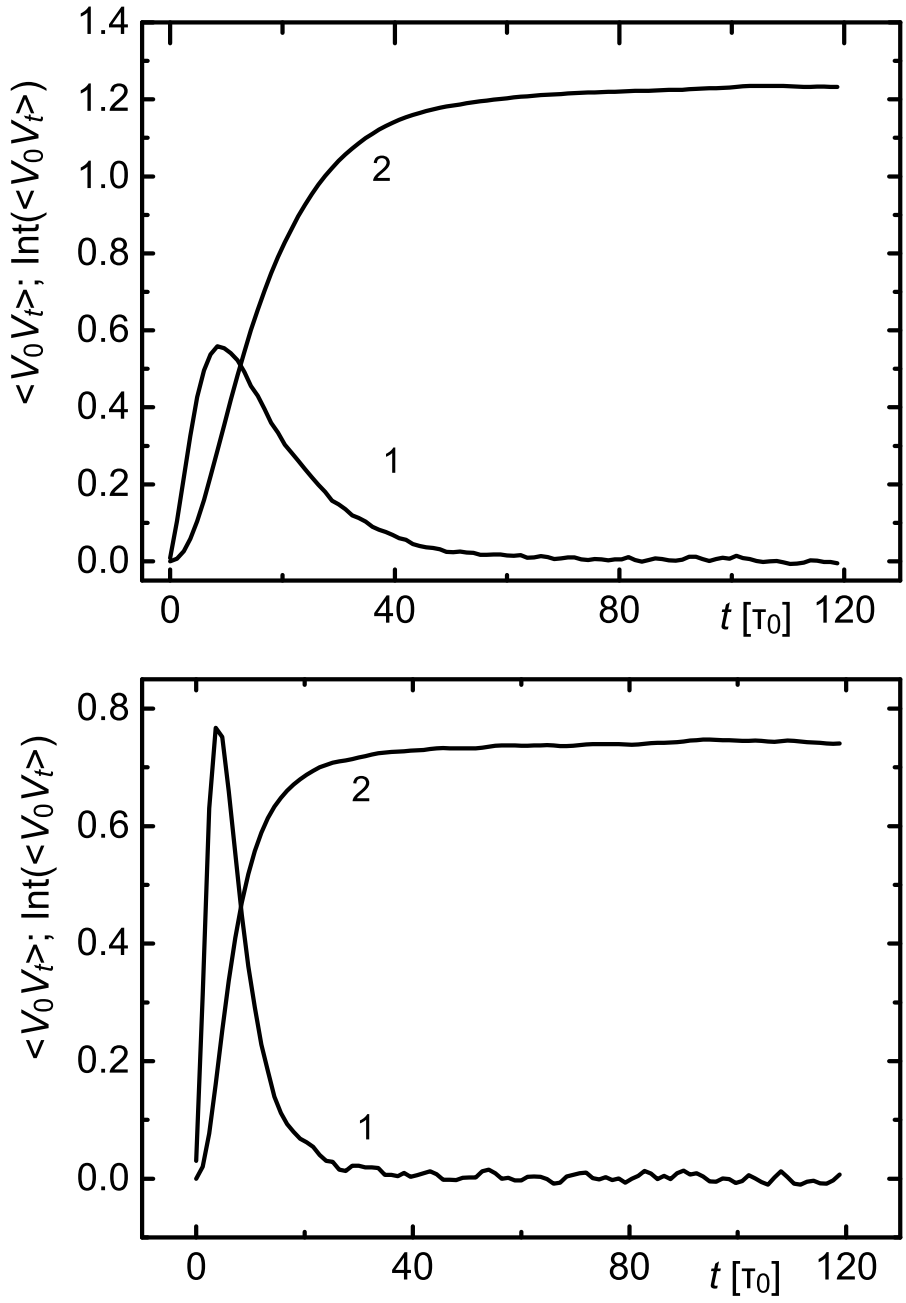

Figure 1. Velocity–velocity autocorrelation functions (lines 1) and their antiderivative functions (lines 2) versus time in atomic units ($\tau_0 = \hbar/\mathrm{Ha}$) for $r_s = 6$, $T = 1.27$ Ha (top panel) and $r_s = 3$, $T = 1.08$ Ha (bottom panel). VVAF are multiplied om 10 for convenience.

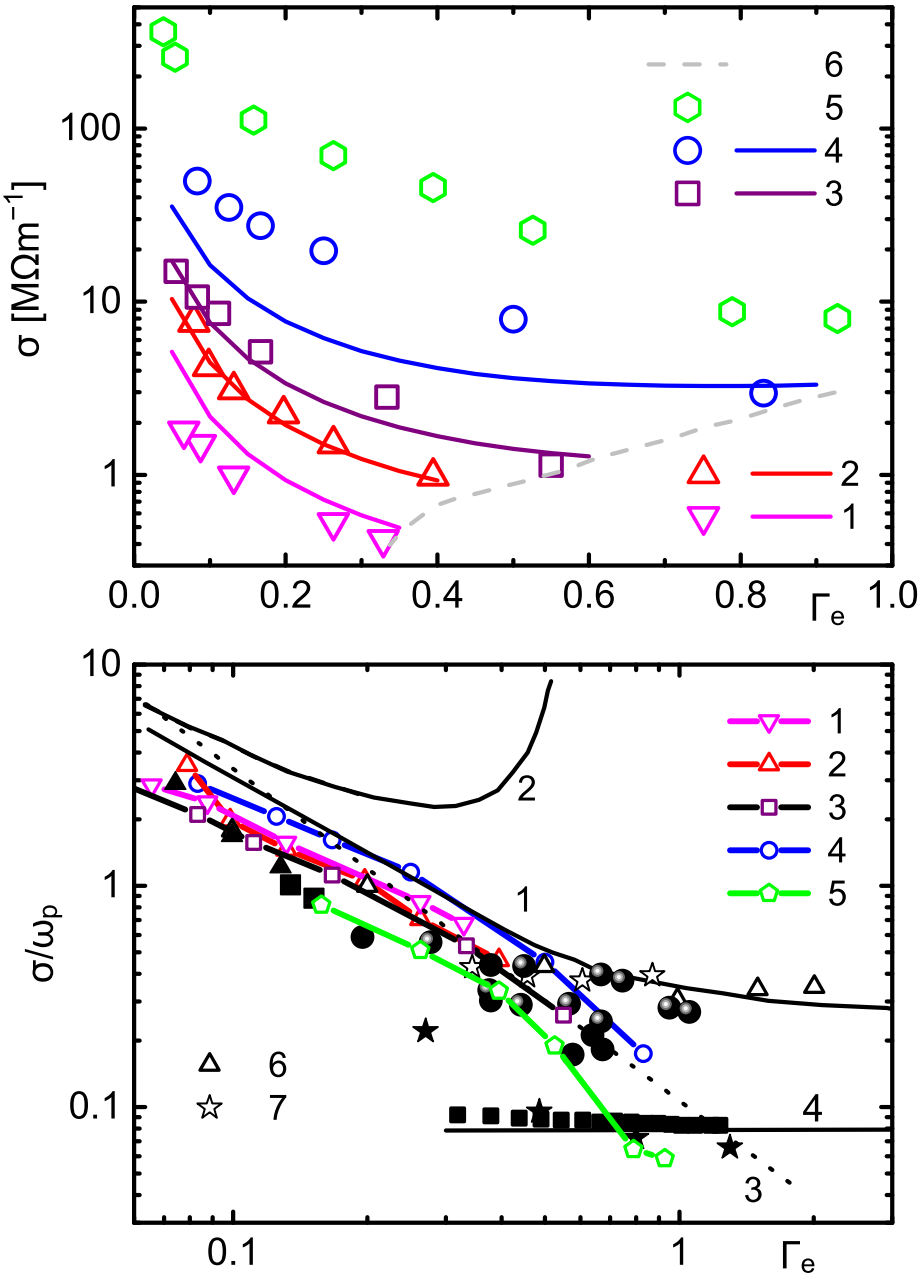

Figure 2. Electrical electron conductivity as function of the coupling parameter Γ_e for different fixed densities of two component Coulomb system. Top panel. Empty scatters: 1–5—show results of this work for fixed $r_s = 6, 4, 3, 2, 1$ respectively, wile related lines present results of interpolation formula for conductivity of fully ionized hydrogen plasma derived in [17, 18]. Line 6 restricts approximately from above the region of conductivity sharp drop due to arising bound states of many particle clusters. Bottom panel. Solid scatters present data of different experiments [3]. Empty scatters: 1–5—illustrate conductivity like on the top panel. Empty scatters: 6–7—present results of theoretical papers [3] and [26] for fully ionized hydrogen plasma. Lines: 1—MD calculations [27]; 2—Landau's formula; 3—Landau's formula at $L_e = 3$; 4—$\frac{1}{4\pi}$.

5 CONCLUSIONS

According to the quantum Kubo formula we have derived a new method for calculation of the electrical conductivity of dense plasma media. This method combines the Feynman and Wigner formulations of quantum mechanics and uses for calculation the direct path integral Monte Carlo and molecular dynamics methods. We applied this method to dense plasma in a wide region of density and temperature. Calculating the momentum–momentum correlation functions we determined the electrical conductivity and compared obtained results with available theories. Our results show a strong dependence on the plasma parameters and for fully ionized plasma are in a good agreement with available theories, simulations, experimental data and interpolation formula obtained by Esser, Redmer and Röpke. Appearing bound states and many particle clusters in plasma results in sharp drop of electron conductivity.

Acknowledgments: The authors thank M. Bonitz and P. Levashov for stimulating discussions and valuable notes. Authors acknowledge the program of fundamental research of the Presidium of the Russian Academy of Sciences "Condensed matter and plasma at high energy densities" for financial support.

The paper is based on the proceedings of the XXXIII International Conference on Equations of State for Matter, which was held in Elbrus and Tegenekli settlements, in the Kabardino-Balkar Republic of the Russian Federation, from March 1 to 6, 2018.

REFERENCES

[1] G. F. Bertsch, M. Bonitz, A. Filinov, V. S. Filinov, Y. Lozovik, D. Semkat, and H. Ruhl, *Introduction to Computational Methods in Many-Body Physics*, Princeton: Rinton Press, (2006).

[2] V. I. Mazhukhin, A. V. Shaprapov, M. M. Demin, A. A. Samokhin, and A. E. Zubko, "Molecular dynamics modeling of nanosecond laser ablation: subcritical regime", *Mathematica Montisnigri* **27**, 24–42 (2016).

[3] I. V. Morozov and G. E. Norman, "Collisions and plasma waves in nonideal plasmas", *J. Exp. Theor. Phys.* **100**, 370 (2005).

[4] A. A. Samokhin, V. I. Mazhukhin, A. V. Shaprapov, M. M. Demin, and P. A. Pivovarov, "Continual and molecular-dynamic modeling of phasetransitions during laser ablation", *Mathematica Montisnigri* **23**, 25–42 (2015).

[5] V. M. Zamalin, G. E. Norman, and V. Filinov, *The Monte-Carlo Method in Statistical Thermodynamics*, Moscow: Nauka, (1977).

[6] V. I. Mazhukhin, A. V. Shaprapov, O. N. Koroleva, and A. V. Rudenko, "Molecular dynamics simulation of critical point parameters for silicon", *Mathematica Montisnigri* **21**, 64–77 (2014).

[7] A. V. Filinov, V. O. Golubnychiy, M. Bonitz, W. Ebeling, and J. W. Dufty, "Temperature-dependent quantum pair potentials and their application to dense partially ionized hydrogen plasmas", *Phys. Rev. E* **70**, 045411 (2004).

[8] N. Schlunzen and M. Bonitz, "Nonequilibrium green functions approach to strongly correlated fermions in lattice systems", *Contrib. Plasma Phys.* **56**, 5 (2016).

[9] K. Balzer and M. Bonitz, *Nonequilibrium Green's Functions Approach to Inhomogeneous Systems*, Springer: Lecture Notes in Physics, vol. 867 (2013), (2013).

[10] D. N. Zubarev, V. Morozov, and G. Ropke, *Statistical Mechanics of Nonequilibrium Processes*, Berlin: Akademie Verlag-Wiley, (1996).

[11] M. Bonitz, *Quantum Kinetic Theory*, Berlin: Springer, (2015).
[12] D. Kremp, M. Schlanges, and W. D. Kraeft, *Quantum Statistics of Nonideal Plasmas*, Berlin: Springer, (2005).
[13] W. Ebeling, V. Fortov, and V. Filinov, *Quantum Statistics of Dense Gases and Nonideal Plasmas*, Berlin: Springer, (2017).
[14] B. Holst, M. French, and R. Redmer, "Electronic transport coefficients from ab initio simulations and application to dense liquid hydrogen", *Phys. Rev. B* **83**, 235120 (2011).
[15] M. P. Desjarlais, C. R. Scullard, L. X. Benedict, H. D. Whitley, and R. Redmer, "Density-functional calculations of transport properties in the nondegenerate limit and the role of electron-electron scattering", *Phys. Rev. E* **95**, 033203 (2017).
[16] V. Zehnle, B. Bernu, and J. Wallenborn, "On the transport properties of a dense fully-ionized hydrogen plasma. I. The semi-classical approach", *Journal de Physique* **49**, 1147 (1988).
[17] A. Esser, R. Redmer, and G. Röpke, "Interpolation formula for the electrical conductivity of nonideal plasmas", *Contrib. Plasma Phys.* **43**, 33 (2003).
[18] J. R. Adams, N. S. Shilkin, V. E. Fortov, V. K. Gryaznov, V. B. Mintsev, R. Redmer, H. Reinholz, and G. Röpke, "Coulomb contribution to the direct current electrical conductivity of dense partially ionized plasmas", *Phys. Plasmas* **14**, 062303 (2007).
[19] V. S. Filinov, H. Fehske, M. Bonitz, V. E. Fortov, and P. R. Levashov, "Correlation effects in partially ionized mass asymmetric electron-hole plasmas", *Phys. Rev. E* **75**, 036401 (2007).
[20] V. Filinov, Yu. Medvedev, and V. Kamskii, "Quantum dynamics and Wigner representation of quantum mechanics", *Molecular Physics* **85**, 711 (1995).
[21] V. S. Filinov, "Wigner approach to quantum statistical mechanics and quantum generalization of molecular dynamics method. Part I", *Molecular Physics* **88**, 1517 (1996).
[22] V. S. Filinov, "Wigner approach to quantum statistical mechanics and quantum generalization of molecular dynamics method. Part II", *Molecular Physics* **88**, 1529 (1996).
[23] A. S. Larkin, V. S. Filinov, and V. E. Fortov, "Peculiarities of momentum distribution functions of strongly correlated charged fermions", *J. Phys. A: Math. Theor.* **51**, 035002 (2018).
[24] V. S. Filinov, B. M, W. Ebeling, and V. E. Fortov, "Thermodynamics of hot dense H-plasmas: Path integral Monte Carlo simulations and analytical approximations", *Plasma Phys. Cont. Fusion* **43**, 743 (2001).
[25] G. Kelbg, "Theorie des quanten-plasmas", *Ann. Physik* **457**, 354 (1963).
[26] E. M. Apfelbaum and M. F. Ivanov, "Calculation of transport coefficients with allowance for the chemical composition of a low-temperature high-density metal plasma.", *Plasma Phys. Rep.* **27**, 76 (2001).
[27] A. A. Valuev and Yu. K. Kurilenkov, *Teplofiz. Vys. Temp.* **21**, 591 (1983).

Received February 5, 2018